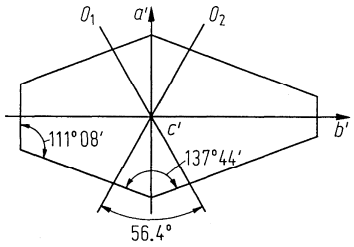

Fig. 31A-3-001. $KH_3(SeO_3)_2$. Crystal form [67Shu]. O_1, O_2: optical axes (λ = 589.0 nm).

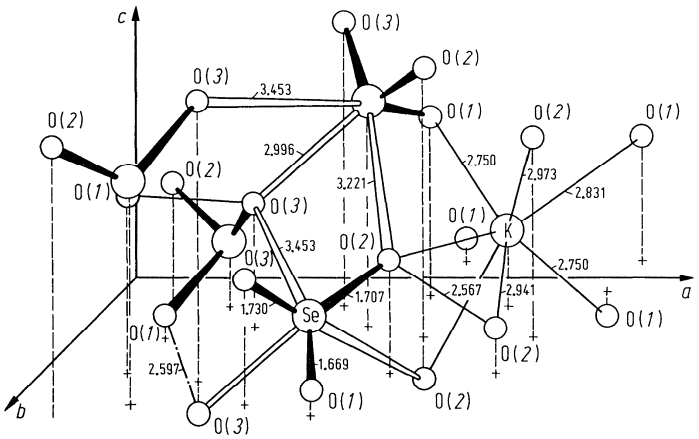

Fig. 31A-3-002. $KH_3(SeO_3)_2$. Crystal structure of phase I [69Han]. Interatomic distances in [Å].

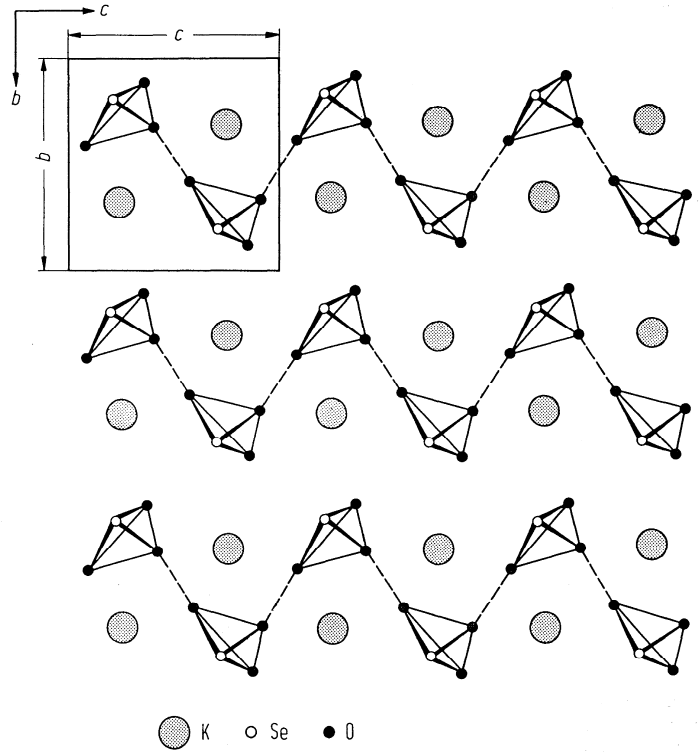

Fig. 31A-3-003. $KH_3(SeO_3)_2$. Crystal structure of phase I [71Gor]. Projection on (100). Dashed lines show the proposed hydrogen bonds.

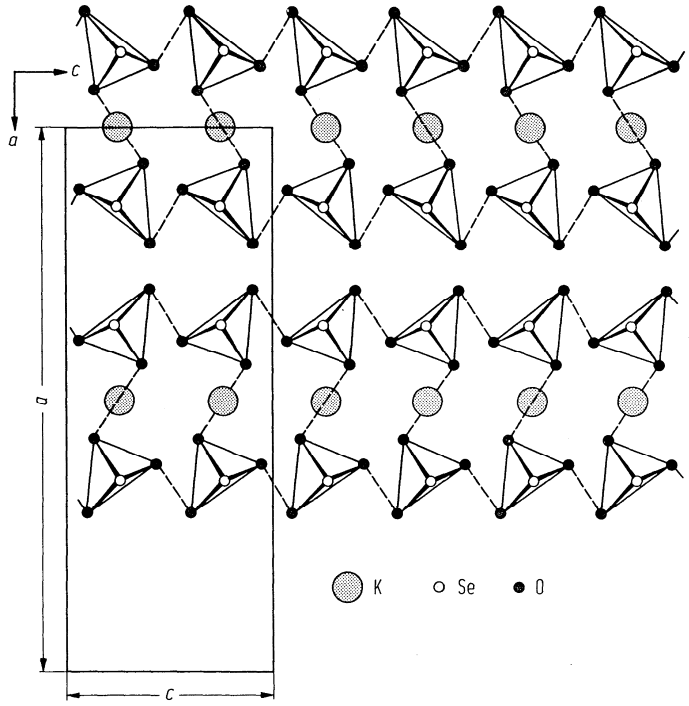

Fig. 31A-3-004. $KH_3(SeO_3)_2$. Crystal structure of phase I [71Gor]. Projection on (010). Dashed lines show the proposed hydrogen bonds.

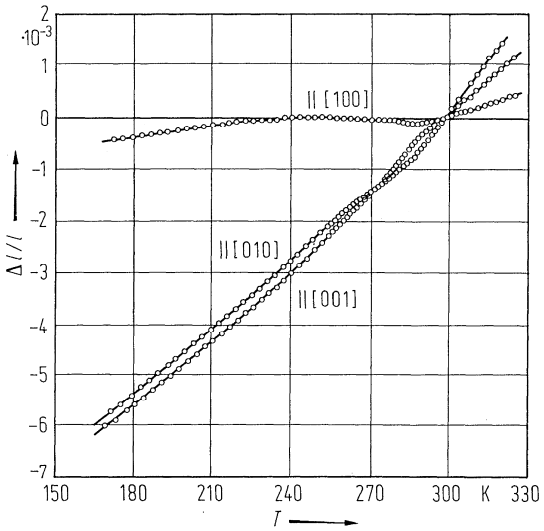

Fig. 31A-3-005. $KD_3(SeO_3)_2$. $\Delta l/l$ vs. T parallel to [100], [010] and [001] [78Mak]. $\Delta l/l$: linear thermal expansion.

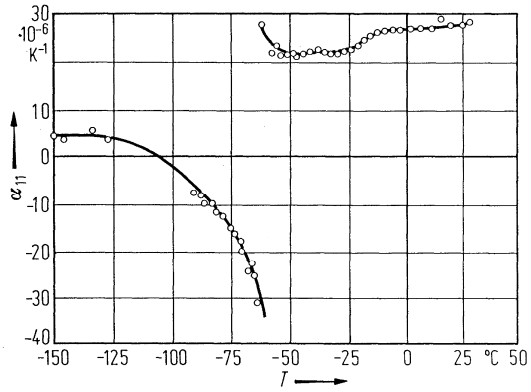

Fig. 31A-3-006. $KH_3(SeO_3)_2$. α_{11} vs. T [71Tiv]. α_{11}: linear thermal expansion coefficient along the a axis.

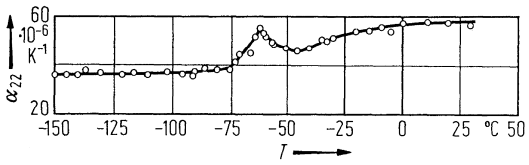

Fig. 31A-3-007. $KH_3(SeO_3)_2$. α_{22} vs. T [71Tiv]. α_{22}: linear thermal expansion coefficient along the b axis.

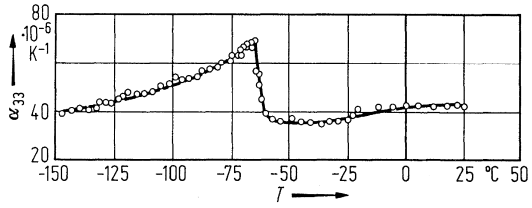

Fig. 31A-3-008. $KH_3(SeO_3)_2$. α_{33} vs. T [71Tiv]. α_{33}: linear thermal expansion coefficient along the c axis.

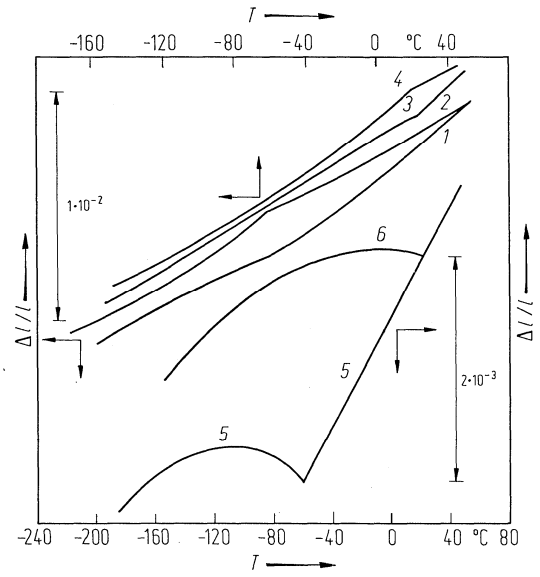

Fig. 31A-3-009. $KH_3(SeO_3)_2$, $KD_3(SeO_3)_2$. $\Delta l/l$ vs. T [79Iva]. $\Delta l/l$: linear thermal expansion. $KH_3(SeO_3)_2$, curve *1*: a axis; curve *2*: b axis; curve *3*: c axis. $KD_3(SeO_3)_2$, curve *4*: a axis; curve *5*: b axis; curve *6*: c axis.

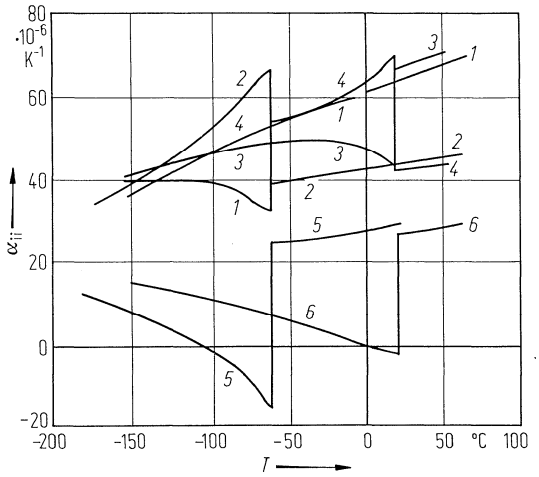

Fig. 31A-3-010. $KH_3(SeO_3)_2$, $KD_3(SeO_3)_2$. α_{ii} vs. T [79Iva]. α_{ii}: linear thermal expansion coefficients. $KH_3(SeO_3)_2$, curve *1*: α_{11}; curve *2*: α_{22}; curve *3*: α_{33}. $KD_3(SeO_3)_2$, curve *4*: α_{11}; curve *5*: α_{22}; curve *6*: α_{33}.

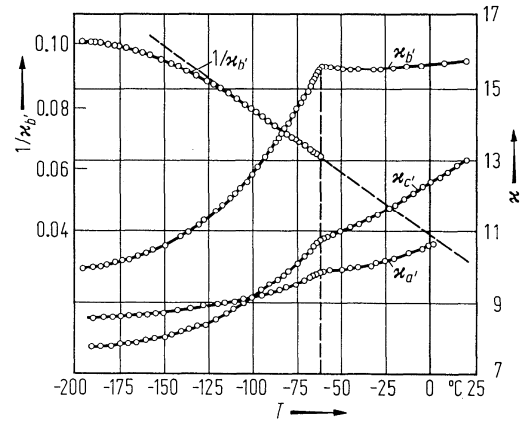

Fig. 31A-3-011. $KH_3(SeO_3)_2$. $\varkappa_a$; $\varkappa_b$; $\varkappa_{c'}$, $1/\varkappa_{b'}$ vs. T [67Shu]. $\varkappa$: low frequency dielectric constant.

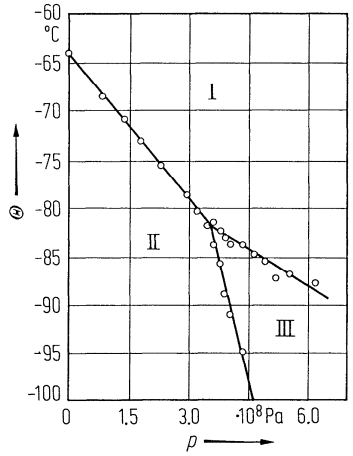

Fig. 31A-3-012. $KH_3(SeO_3)_2$. Θ vs. p [73Ges].

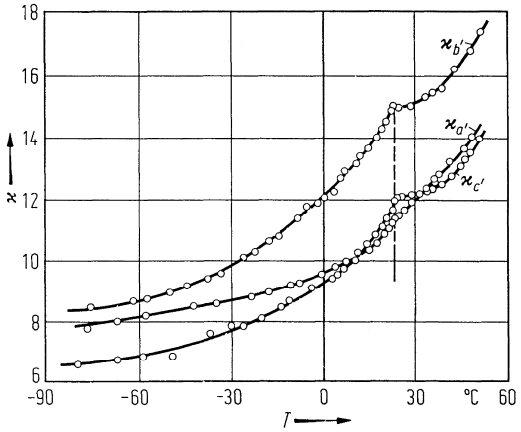

Fig. 31A-3-013. $KD_3(SeO_3)_2$. κ_a; κ_b; $\kappa_{c'}$ vs. T (f = 2 kHz) [69Yag].

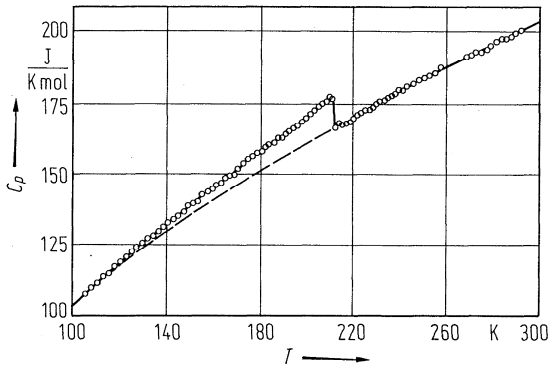

Fig. 31A-3-014. $KH_3(SeO_3)_2$. C_p vs. T [77Mak2].

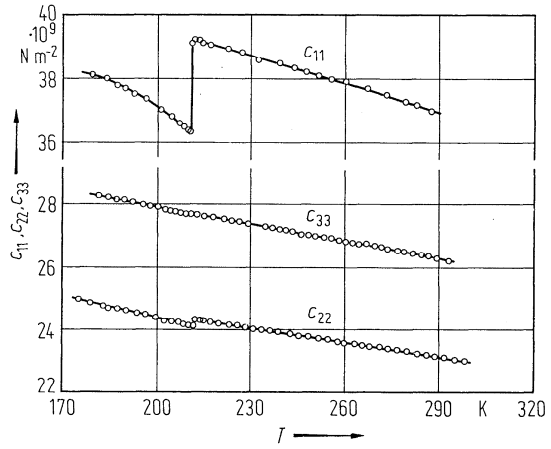

Fig. 31A-3-015. $KH_3(SeO_3)_2$. c_{11}, c_{22}, c_{33} vs. T [77Mak1].

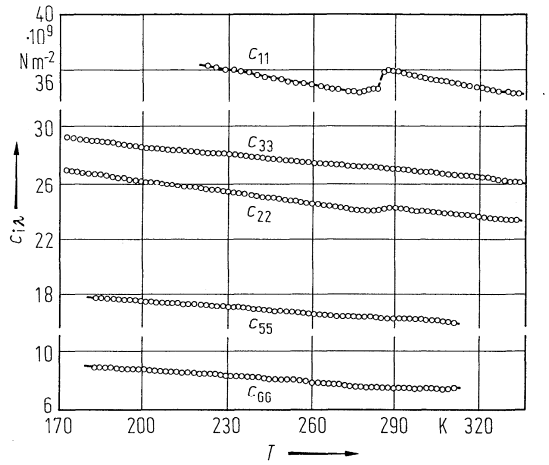

Fig. 31A-3-016. $KD_3(SeO_3)_2$. $c_{i\lambda}$ vs. T [78Mak]. f = 10 MHz for longitudinal waves. f = 5 MHz for transverse waves.

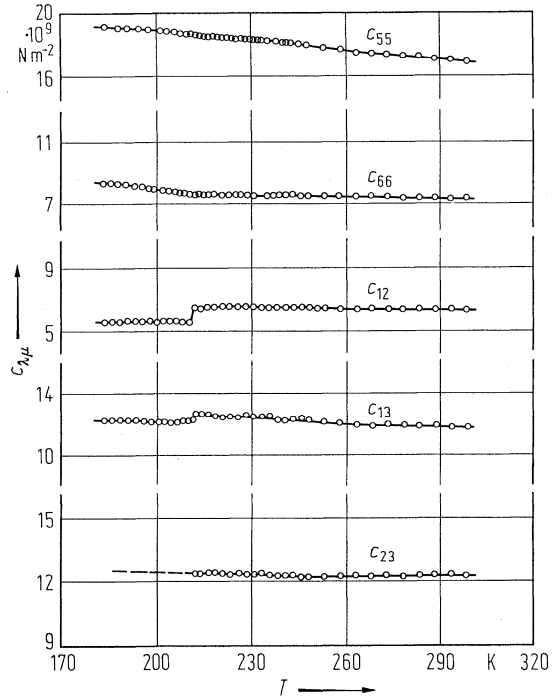

Fig. 31A-3-017. $KH_3(SeO_3)_2$. c_{55}, c_{66}, c_{12}, c_{13}, c_{23} vs. T [77Mak1].

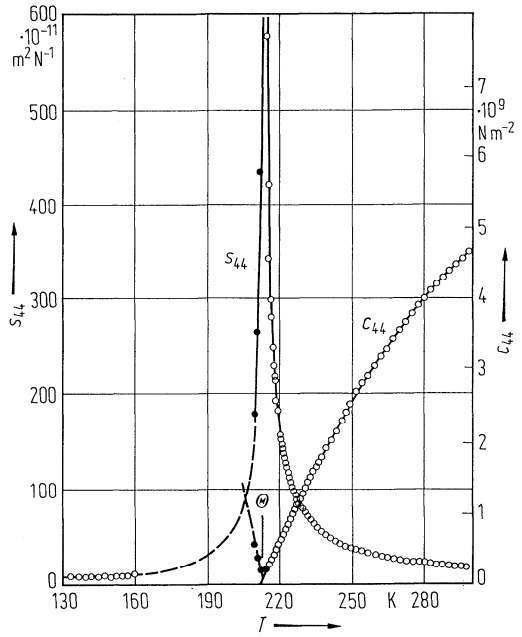

Fig. 31A-3-018. $KH_3(SeO_3)_2$. s_{44}, c_{44} vs. T [77Mak1].

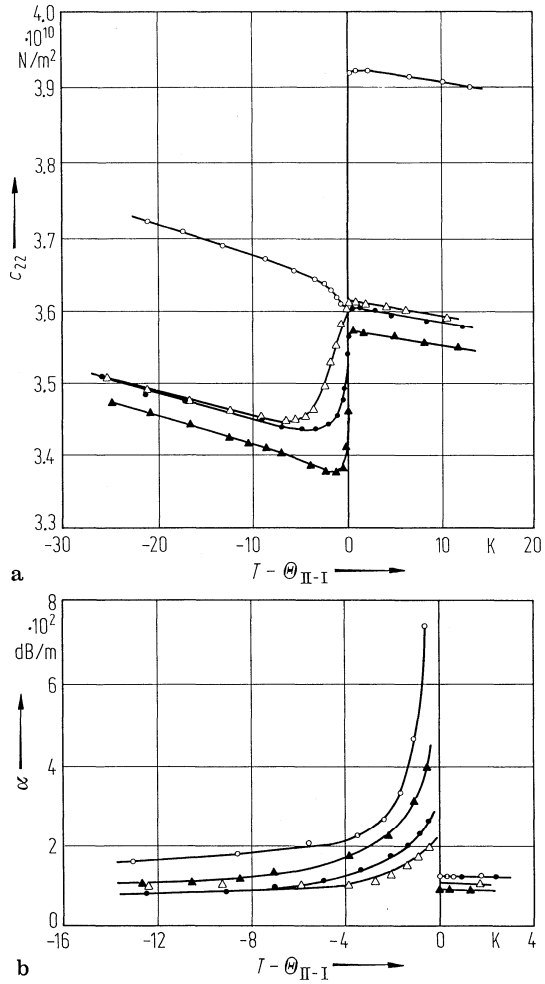

Fig. 31A-3-019. $K(H_{1-x}D_x)_3(SeO_3)_2$. c_{22}, α vs. $T - \Theta_{II-I}$ [82Sor1]. f = 20 MHz. Open circle: x = 0.0, open triangle: x = 0.81, full circle: x = 0.87, full triangle: x = 0.97; (**a**) c_{22} vs. $T - \Theta_{II-I}$; (**b**) α vs. $T - \Theta_{II-I}$. α: attenuation coefficient of the corresponding longitudinal sound.

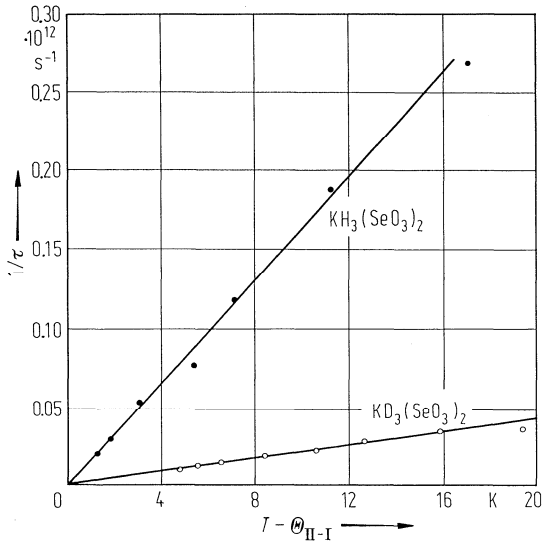

Fig. 31A-3-020. $KH_3(SeO_3)_2$, $KD_3(SeO_3)_2$. $1/\tau$ vs. $T-\Theta_{II-I}$ [84Gar]. τ: critical relaxation time deduced from the ultrasonic measurements. $f \approx 10\ldots50$ MHz.

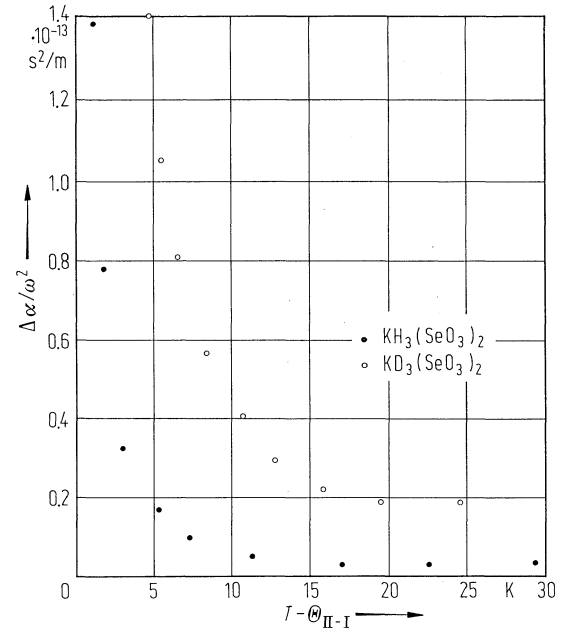

Fig. 31A-3-021. $KH_3(SeO_3)_2$, $KD_3(SeO_3)_2$. $\Delta\alpha/\omega^2$ vs. $T - \Theta_{II-I}$ [84Gar]. $\Delta\alpha$: anomalous part of the sound attenuation coefficient. $f \approx 10$ MHz.

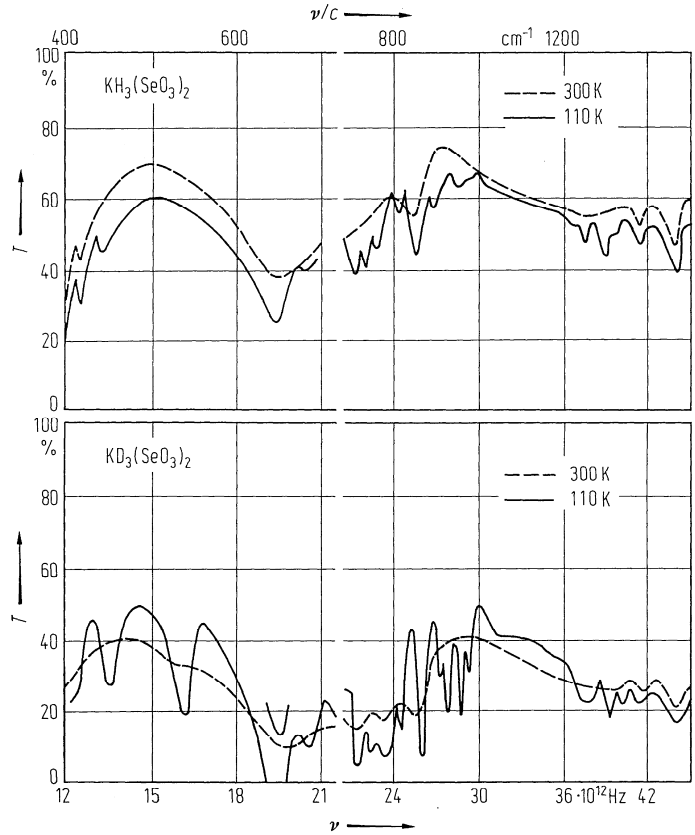

Fig. 31A-3-022. $KH_3(SeO_3)_2$, $KD_3(SeO_3)_2$. T vs. ν [73Ach]. T: transmission of the infrared radiation. The deuterium content is estimated to be more than 80%.

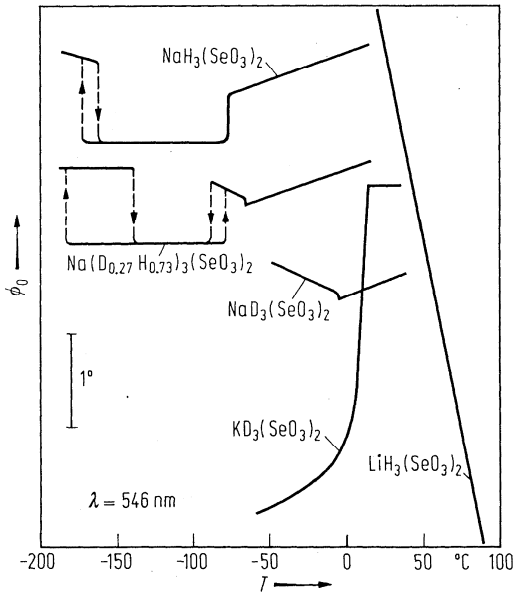

Fig. 31A-3-023. $LiH_3(SeO_3)_2$, $NaH_3(SeO_3)_2$, $NaD_3(SeO_3)_2$, $Na(D_{0.27}H_{0.73})_3(SeO_3)_2$, $KD_3(SeO_3)_2$. ϕ_0 vs. T [70Iva]. ϕ_0: rotation angle of the optical indicatrix around the b' axis.

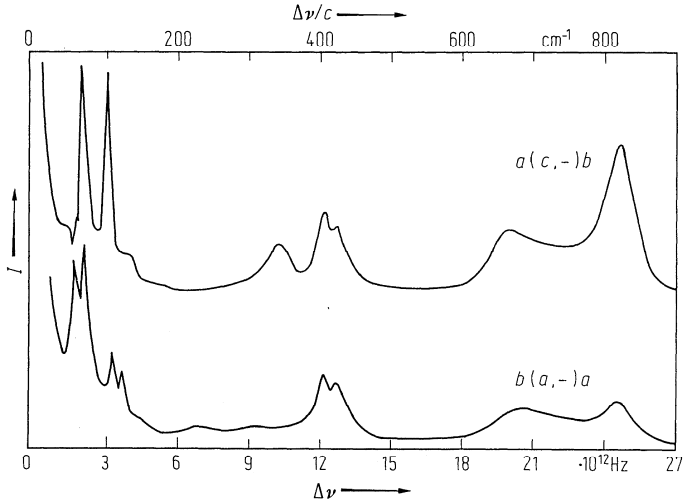

Fig. 31A-3-024. $KH_3(SeO_3)_2$. I vs. $\Delta\nu$ [73Ach]. I: Raman scattering intensity at RT. Hyphens in the notation of the scattering geometry mean that the polarization of light is not specified.

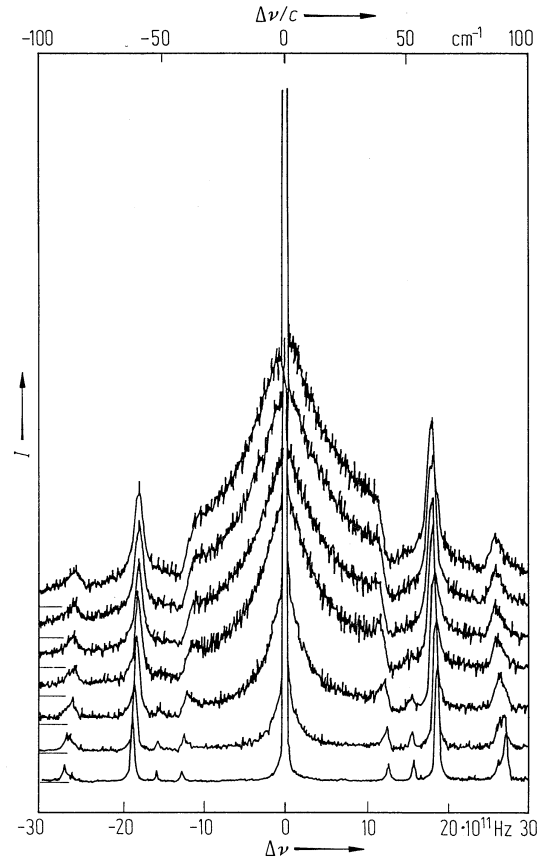

Fig. 31A-3-025. $KH_3(SeO_3)_2$. I vs. $\Delta\nu$ [83Tan]. $\Delta\nu$: Rayleigh wing of B_{3g} symmetry mode. Parameter: T, from the top to the bottom: –61.9, –64.7, –69.4, –78.6, –101.2, –128.4, –158.7 °C.

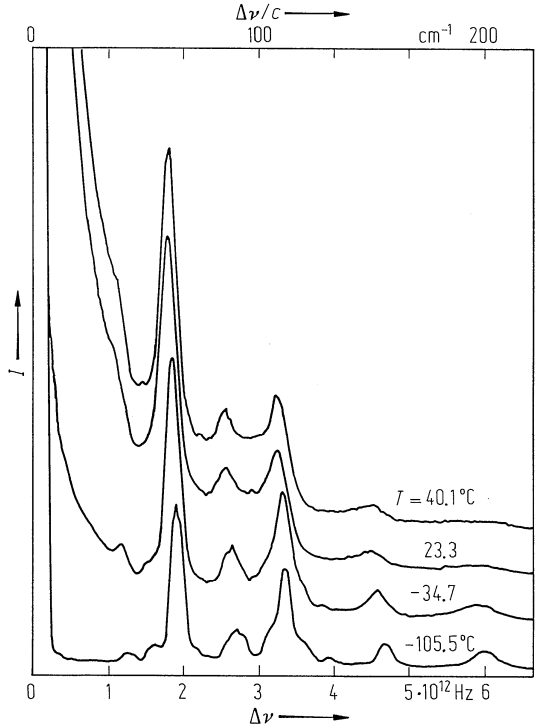

Fig. 31A-3-026. $KD_3(SeO_3)_2$. I vs. $\Delta\nu$ [84Tat]. I: Raman scattering intensity for the scattering geometry $Z(YZ)Y$. Parameter: T.

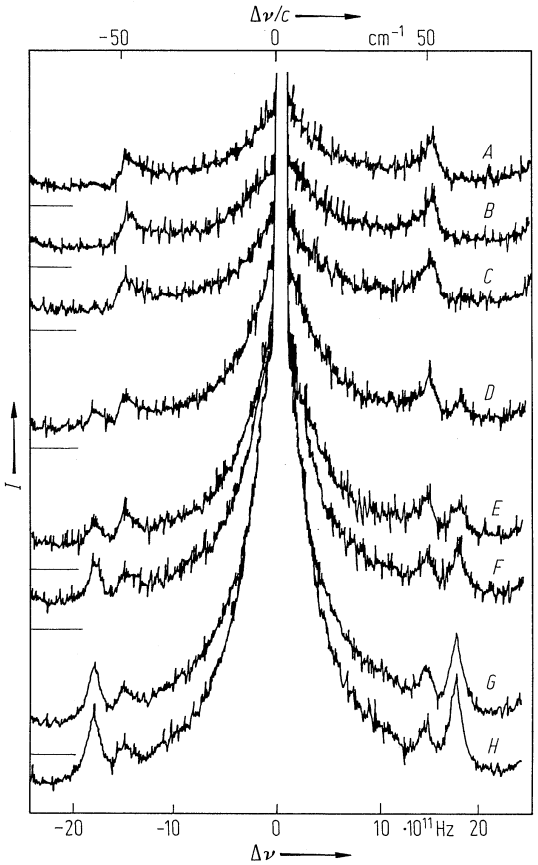

Fig. 31A-3-027. $KD_3(SeO_3)_2$. *I* vs. $\Delta\nu$ [84Tan]. Parameter: *T*. *I*: intensity of low frequency Raman spectra in *X*(*YY*)*Z* scattering geometry. Θ_{II-I} = 28.9 °C, *A*: 32.21 °C, *B*: 30.65 °C, *C*: 29.39 °C, *D*: 28.90 °C, *E*: 28.80 °C, *F*: 28.50 °C, *G*: 27.63 °C, *H*: 26.86 °C.

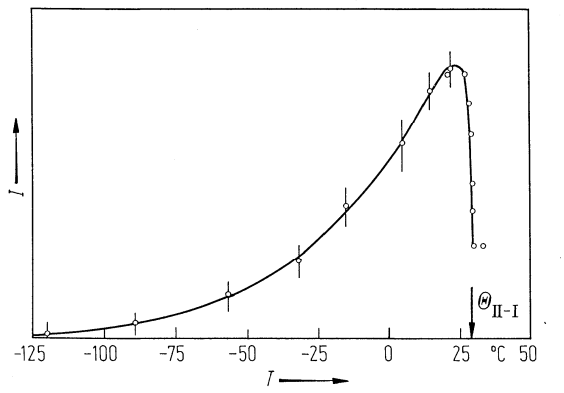

Fig. 31A-3-028. $KD_3(SeO_3)_2$. *I* vs. *T* [84Tan]. *I*: intensity of Rayleigh wing in *X*(*YY*)*Z* scattering geometry.

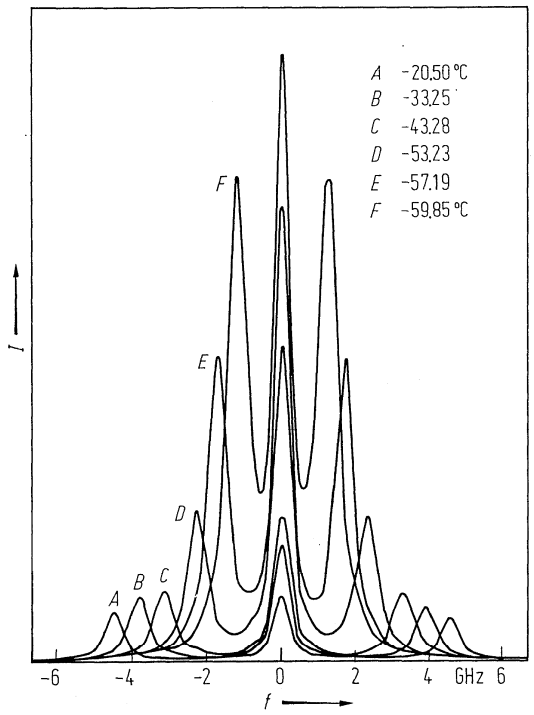

Fig. 31A-3-029. $KH_3(SeO_3)_2$. *I* vs. *f* [77Yag1]. *I*: Brillouin spectra associated with the soft acoustic mode s_{44} observed for as-grown crystal.

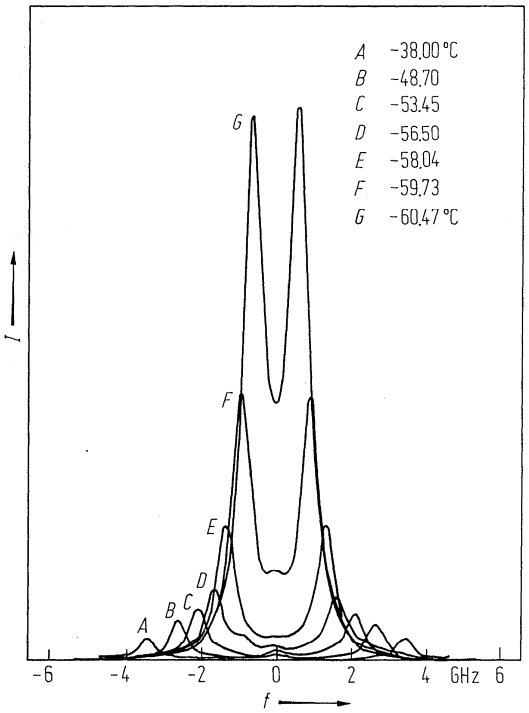

Fig. 31A-3-030. $KH_3(SeO_3)_2$. *I* vs. *f* [77Yag1]. *I*: Brillouin spectra associated with the soft acoustic mode s_{44} observed after repeated measurements.

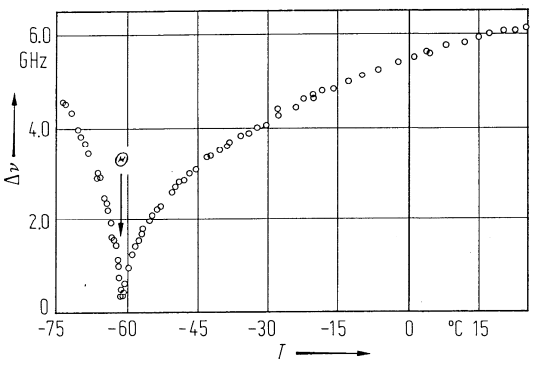

Fig. 31A-3-031. $KH_3(SeO_3)_2$. $\Delta\nu$ vs. T [77Yag2]. $\Delta\nu$: Brillouin shift of c_{44} mode. $\lambda = 488.0$ nm.

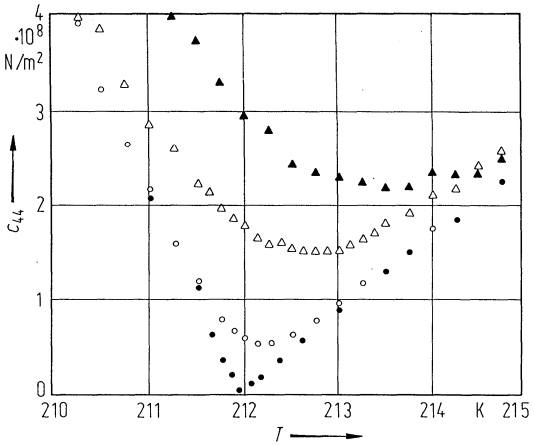

Fig. 31A-3-032. $KH_3(SeO_3)_2$. c_{44} vs. T [81Cop]. Parameter: T_{44}. Full circle: $T_{44} = 0$, open circle: $163 \cdot 10^3$ N m^{-2}, open triangle: $325 \cdot 10^3$ N m^{-2}, full triangle: $442 \cdot 10^3$ N m^{-2}.

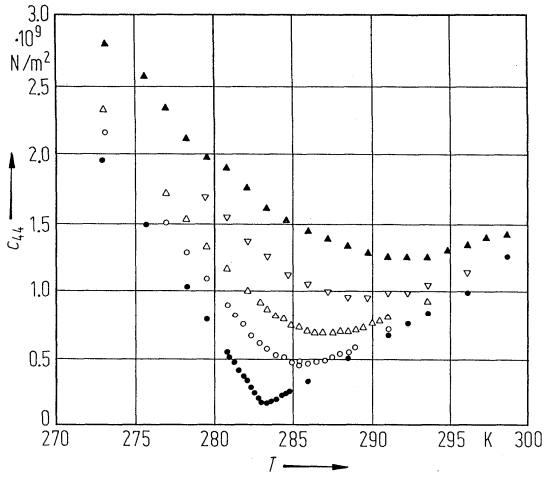

Fig. 31A-3-033. $KD_3(SeO_3)_2$. c_{44} vs. T [81Cop]. Parameter: T_{44}. Full circle: $T_{44} = 0$, open circle: $710 \cdot 10^3$ N m^{-2}, open upside triangle: $1400 \cdot 10^3$ N m^{-2}, open downside triangle: $2400 \cdot 10^3$ N m^{-2}, full triangle: $3800 \cdot 10^3$ N m^{-2}.

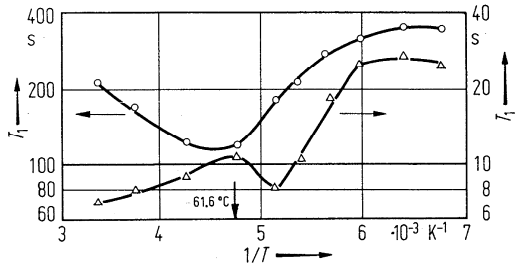

Fig. 31A-3-034. $KH_3(SeO_3)_2$. T_1 vs. 1/T [71Sil]. T_1: spin-lattice relaxation time of proton. Relaxation time was measured for single crystal. $\boldsymbol{H} \parallel \boldsymbol{a}$. The two T_1 values are attributed to two nonequivalent sites of hydrogens.

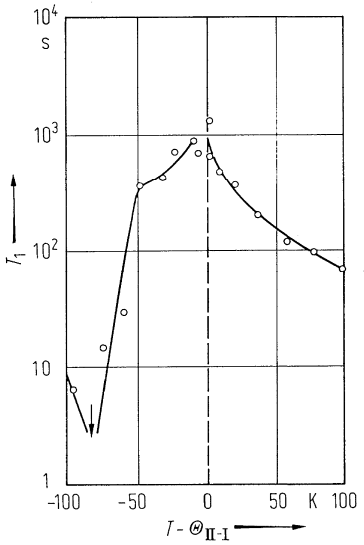

Fig. 31A-3-035. $KH_3(SeO_3)_2$. T_1 vs. $T - \Theta_{II-I}$ [78Sla]. T_1: proton spin-lattice relaxation time. Magnetic field = $21.48 \cdot 10^3$ A m^{-1}.

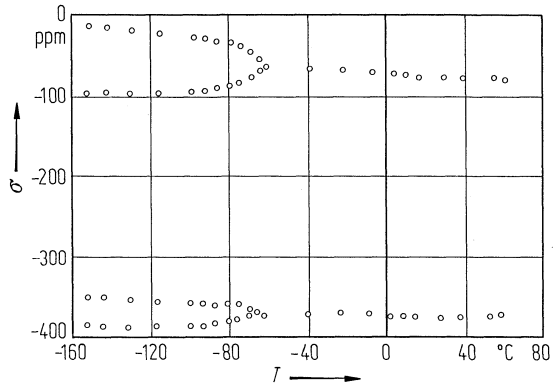

Fig. 31A-3-036. $KH_3(SeO_3)_2$. σ vs. T [80Suk]. σ: chemical shift of the ^{77}Se nuclei. $\boldsymbol{H} \perp \boldsymbol{c}$. $\angle(\boldsymbol{H}, \boldsymbol{a}) = 45°$.

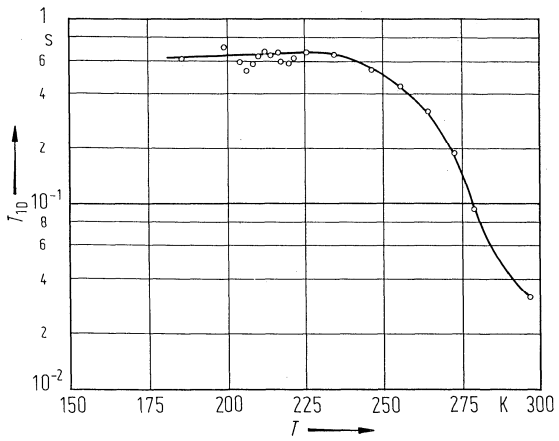

Fig. 31A-3-037. $KH_3(SeO_3)_2$. T_{1D} vs. T [81Bli]. T_{1D}: proton spin-lattice relaxation time in dipolar field.

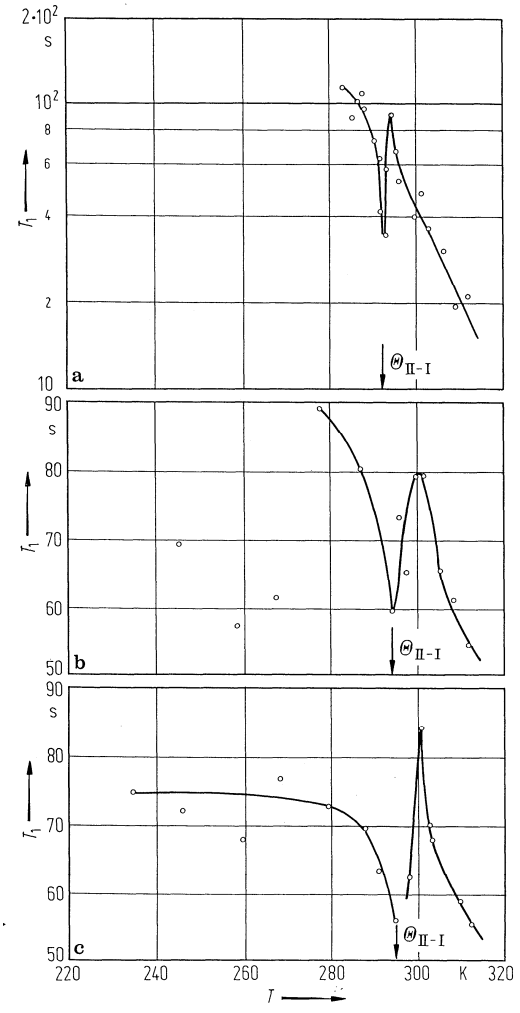

Fig. 31A-3-038. $KD_3(SeO_3)_2$. T_1 vs. T [81Bli]. T_1: deuteron spin-lattice relaxation time. (**a**) ν_L = 13.4 MHz. D(2). (**b**) ν_L = 41 MHz. D(2). (**c**) ν_L = 41 MHz. D(1).

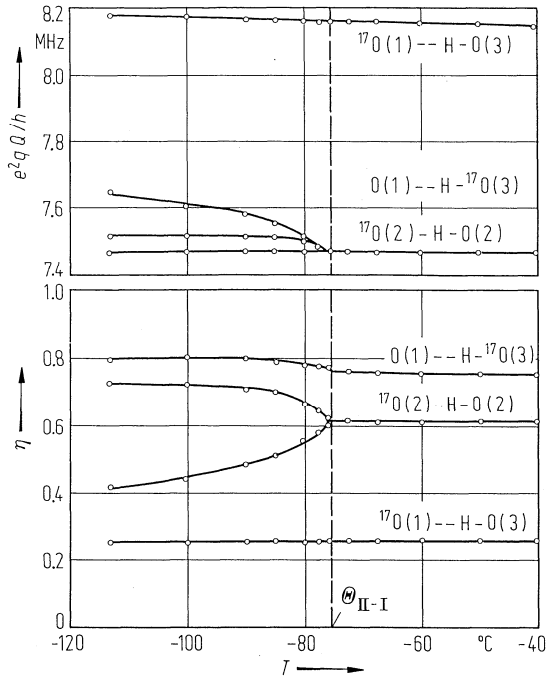

Fig. 31A-3-039. $KH_3(SeO_3)_2$. e^2qQ/h, η vs. T [86Sel]. e^2qQ/h: ^{17}O nuclear quadrupole coupling constant. η: asymmetry parameter.

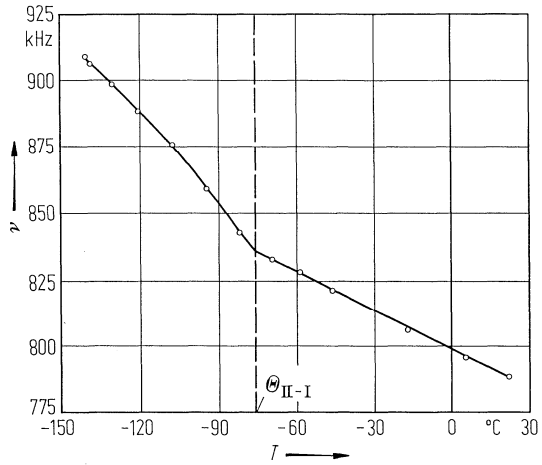

Fig. 31A-3-040. $KH_3(SeO_3)_2$. ν vs. T [86Sel]. ν: NQR frequency of ^{39}K.